EFFECT OF GROUNDWATER LEVEL VARIATION ON THE BEHAVIOR OF PILED RAFT IN CLAY SOIL

Rajib Modak*[1] and Baleshwar Singh[2]

[1] *Research Scholar, Indian Institute of Technology Guwahati, India, e-mail: rajibmodak58987@gmail.com*
[2] *Professor, Indian Institute of Technology Guwahati, India, e-mail: baleshwar@iitg.ac.in*

***Corresponding Author**

ABSTRACT

Piled raft foundation has proven to be a cost-effective foundation option compared to conventional foundation types in terms of bearing capacity and settlement perspectives. The overall behavior of the PRF is affected by the variation in the groundwater level (GWL) as it changes the effective stress conditions of the soil. Three-dimensional finite element analyses have been conducted to study the effect of drawdown in GWL on the behavior of large PRF in stiff clay soil after the application of total superstructure load. To simulate the construction phase, the total load is applied over a period of time in increments. Thereafter, for simulating the GWL drawdown, the finite element model incorporates a fully coupled flow-deformation analysis that takes account of the simultaneous development of deformations and pore water pressures. The number, spacing, and length of piles are varied along with raft thickness. The raft thickness is altered so that the raft-soil stiffness varies as fully flexible, flexible and rigid. The effect of varying the foundation parameters and GWL drawdown on the PRF response is investigated in terms of settlement, bending moment of raft, load-sharing, and axial load distribution of piles. Results show that due to the drawdown in GWL, the average settlement increases for all configurations with varying pile number, pile spacing, pile length, and raft thickness. However, the increase in the settlement value is the minimum for a lower pile number or lower pile spacing and is similar for piled raft configurations with varying pile lengths or raft thicknesses. Both positive and negative raft bending moments reduce noticeably due to the GWL drawdown. The percentage reduction in bending moment of raft is noted to be the most for configurations with a greater pile number, longer pile length, or a raft of greater stiffness. For all the configurations, a drop in the GWL results in an increased proportion of load carried by the piles. The increase in the pile load proportion is the lowest for configurations with a lesser number of piles or shorter-length piles. The axial load carried by the piles at the middle, edge, and corner locations in the pile group increases due to the GWL drawdown for configurations with a higher pile number, wider pile spacing, or longer-length piles.

Keywords: *Large piled raft, groundwater level, fully coupled flow-deformation analysis, numerical modeling, clay soil*

1. INTRODUCTION

A raft and a pile group make up a piled raft foundation, a composite construction that carries the superstructure load via raft-soil contact stress, and pile friction resistance and end bearing. Because piled rafts have benefits over conventional deep or shallow foundations in terms of bearing capacity and settlement considerations, their application has been gaining increasing recognition (Poulos, 2001; El-Mossallamy, 2002). Small and large piled rafts are the two groups into which Russo and Viggiani (1998) have classified them. In the case of small piled rafts, added piles can give a sufficient safety factor for bearing capacity and to minimize settlement, as the unpiled raft bearing capacity is inadequate to support the superstructure load with a suitable safety factor. Small piled raft often has raft width (B_r) that is lesser than the pile length (L_p) ($B_r/L_p < 1$). However, large piled raft is one with the raft having sufficient bearing capacity to support the total load applied with sufficient safety factor, and thus added piles essentially minimize settlement. The raft width in this instance is comparatively greater than the pile length ($B_r/L_p > 1$). Complex interactions between the raft, soil, and piles determine the proportion of the total load carried by individual structural components, *i.e*., raft and piles (Katzenbach *et al*., 2000). The variation in the groundwater level (GWL) can affect the load-carrying behavior of the raft and piles due to the change in the effective stress conditions of the soil. The variations in GWL can be attributed to seasonal fluctuations due to precipitation or excessive groundwater extraction. The variation in the GWL also results in substantial settlement that can exceed the permissible limit, thus causing damage to the superstructure.

Several studies have investigated the effect of GWL fluctuations on the behavior of foundations (Georgiadis *et al*., 2003; Shahriar *et al*., 2013; Park *et al*., 2017; Al-Khazaali and Vanapalli, 2019; Roh *et al.,* 2019; Phoban *et al*., 2021). According to Georgiadis *et al*. (2003), who investigated single pile behavior in partially saturated conditions, single pile settlement is dependent upon changes in the matric suction or capillary stress that correspond to the position of the GWL. In laboratory experiments, Shahriar *et al*. (2013) assessed the impact of the rise in the GWL on the settlement of shallow foundations resting on granular soils and found that the saturation of the soil beneath the footing significantly increased the settlement. Park *et al*. (2017) carried out model load testing for shallow foundations in sands using a hydraulically controlled system, and proposed design equations and correlation parameters for the bearing capacity and settlement as a function of GWL, applied load, and relative density. Al-Khazaali and Vanapalli (2019) examined the behavior of a single model pile and pile groups in sand by varying the GWL and reported that settlements significantly decreased as a result of matric suction, while the ultimate bearing capacity of the foundations increased by 2 to 2.5 times when compared to fully saturated condition. Roh *et al.* (2019) investigated the load-settlement and axial load capacity of piled rafts for various levels of groundwater using three-dimensional finite element analysis and proposed GWL effect factors for load capacity and settlement as a function of GWL depth. In order to protect existing structures, Phoban *et al*. (2021) evaluated the behavior of pile foundations as a result of a rise in the GWL using two-dimensional finite element analysis and suggested guidelines for assessing pile stability during the GWL increase.

Most studies have reported on delineating the effect of GWL variations on the traditional shallow and deep foundations. The influence of the GWL fluctuations on the behavior of piled raft foundations has not received much attention. For piled rafts, due to the complex raft-soil-pile interactions and different influence zones of the individual structural components, the effect of GWL fluctuations needs to be addressed in detail for an efficient design. Moreover, only a few studies have taken account of the presence of partially saturated zones above the GWL location. Ignoring the increase in the shear strength of the soil above the GWL due to matric suction results in a conservative design. For this study, three-dimensional numerical modeling has been carried out to investigate the effect of continuous drawdown in GWL for a certain period on large PRF behavior in stiff clay soil after applying total superstructure load in terms of settlement, raft bending moment, load-sharing between raft and piles, and pile axial load. The number, spacing, and length of piles are varied along with raft thickness. The finite element model incorporates fully coupled flow-deformation analysis that takes account of the partially saturated soil and suction above the GWL location.

2. NUMERICAL STUDY

3. Finite element modeling and constitutive model

The finite element-based program Plaxis 3D has been used to do three-dimensional (3D) numerical modeling (Brinkgreve *et al*., 2015). The soil has been modeled with 10-noded tetrahedral elements, whereas the raft is represented with 6-noded triangular plate elements. Twelve-noded interface elements are utilized to represent the interaction between the soil and the raft. At the start of the analysis, the piles are presumed to be stress-free since they are considered bored piles. To model the pile and to simulate the interaction between the soil at the pile base and along the side, 3-noded embedded beam elements which are made up of special interface elements are employed. In order to avoid any unwanted boundary effects, domain analysis is performed to determine the domain size. At the lateral boundaries, soil displacement is allowed in the vertical direction but restricted in the horizontal direction. In contrast to the ground surface, where soil displacement can occur in all directions, the bottom boundary restricts soil displacement in all directions. Three times the width of raft (B_r) from its edges in the lateral direction and five times the width (B_r) from the base of pile in the vertical direction are chosen as the soil model boundaries based on the domain analysis. The hydraulic boundary conditions are adopted such that the side boundaries and the top surface of the soil model are kept open, but the bottom of the soil model is closed. The open side boundaries indicate the flow of water both inwards and outwards. The considered hydraulic conditions ensure the transient water flow in the partially saturated zone of the soil above the GWL. Following the determination of the boundaries of the soil domain, fine mesh is globally selected to model the soil domain. Local mesh refinement has been applied in the vicinity of the structural components (raft and piles), based on mesh convergence analysis. Figure 1 displays a typical soil domain finite element mesh together with the piled raft foundation.

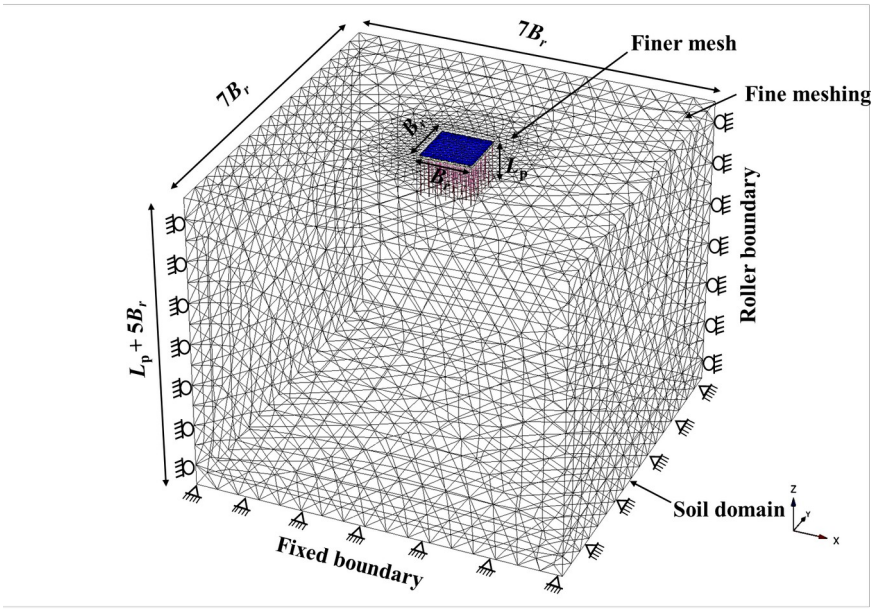

Figure 1: Soil domain and piled raft finite element mesh

The Hardening soil model that incorporates both shear hardening and compression hardening has been adopted to simulate the elastoplastic soil behavior (Brinkgreve *et al*., 2015). In this model, three elastic moduli values are used as input parameters. The real soil behavior is replicated as the soil plasticity happens prior to failure criterion is achieved. Since raft and piles have much higher Young's modulus than the soil, they are considered to show linear elastic behavior. The drawdown of the GWL is simulated in Plaxis 3D by employing the fully coupled flow-deformation function that includes Biot's theory of 3D consolidation (Biot 1941). The function is based on small strain theory, and Darcy's law is valid for fluid flow. In addition, this function considers the simultaneous development of pore water pressures and deformations in soils incorporating the nonlinear elastoplastic behavior and soil-water retention properties in partially or fully saturated conditions following time-dependent hydraulic boundary conditions.

4. Numerical model validation

For validating the numerical modeling in Plaxis 3D, the current study results are compared with those stated by Cho *et al*. (2012). A square raft of 10 × 10 m and 1 m thick has been taken into consideration for this purpose. Nine piles overall, with diameter of 0.5 m and length ranging from 8 to 20 m, are positioned in a square pattern of 3 × 3 configuration. The spacing between the piles adopted are three times the pile diameter. Table 1 lists the material properties of the raft, piles, and soil used in the validation. Figures 2a and 2b respectively illustrate the comparison of the load-average settlement and load-differential settlement plots, obtained using Plaxis 3D and as reported by Cho *et al*. (2012). It can be noted that the current study results correspond well with the published results.

Table 1: Properties of materials used for validation

Parameters	Raft	Piles	Stiff clay	Bearing layer
Modulus of elasticity, E' (MPa)	30,000	12,500	45	500
Cohesive strength, c' (kPa)	--	--	20	0.1
Friction angle, ϕ' (°)	--	--	20	45
Poisson's ratio, ν'	0.20	0.25	0.3	0.3
Unit weight, γ_t (kPa)	25	25	19	20
Model	Elastic	Elastic	Mohr-Coulomb	Mohr-Coulomb

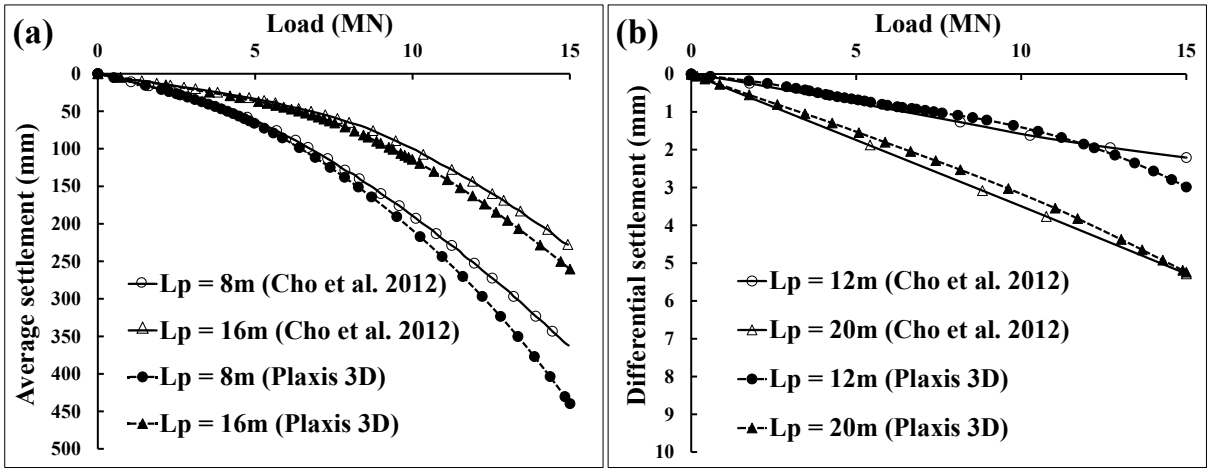

Figure 2: Comparison of the load-settlement behavior obtained in Plaxis 3D with the results reported by Cho *et al*. (2012): (a) average; and (b) differential settlement

5. Parametric analyses

For this study, a flexible square raft with a size of 38 × 38 m sitting on stiff clay soil is studied. Three-dimensional numerical studies with varying number, spacing, and length of piles along with the change in raft thickness are performed. The ranges of the different foundation parameters are presented in Table 2. The various pile configurations used in the investigation are depicted in Figure 3. As seen in Figures 3a, 3b, and 3c, the pile numbers are changed to 25, 49, and 81 such that the area covered by the piles is maximum. The fraction of area covered by the group of piles (A_g) to total area of the raft (A_r) is termed the piled area ratio (A_g/A_r) indicates the area the pile group covers. The corresponding 25, 49, and 81 piles are positioned in a square arrangement as 5 × 5, 7 × 7, and 9 × 9 configurations. The A_g/A_r ratio, while varying the pile number, is kept constant at 0.9. The ratio of pile spacing to the pile diameter (s/D_p) is varied as 4, 5, and 6, with the corresponding A_g/A_r ratios of 0.4, 0.6, and 0.9, as illustrated in Figures 3c, 3d, and 3e. The pile length to diameter ratios (L_p/D_p) are considered as 20, 25, and 30. According to Fraser and Wardle (1976), dependent on the raft-soil stiffness ratio (k_{rs}), the various raft thicknesses are taken into account to ensure that the raft stiffness varies from fully flexible, flexible, and rigid. The pile diameter (D_p) of 1 m has been kept constant throughout the study. For the other parameters, the standard values listed in Table 2 are taken into

account when varying a specific foundation parameter. From Engin and Brinkgreve (2009) and Katzenbach *et al*. (2000), for the stiff clay soil type under consideration, the parameters of the Hardening soil material and the geotechnical properties are taken. The properties of the structural elements are taken from Reul and Randolph (2004). The material characteristics of the soil, raft, and piles used in the investigation are shown in Table 3. The piles are considered as bored concrete piles and since a majority of load is carried through frictional resistance, the piles can be termed as friction piles. Plaxis 3D incorporates Mualem-Van Genuchten functions to describe the flow behavior in the unsaturated zone. The unsaturated flow parameters in these functions for clay soil type classified based on the USDA soil classification (Carsel and Parrish, 1988) are mentioned in Table 3.

The finite element analysis consists of three phases. In the first phase (initial phase), the soil domain is activated, which basically involves calculating the initial stress field for the initial geometry configuration. This is followed by the loading phase, where the piled raft is activated, and uniformly distributed load (*UDL*) up to 150 kPa is applied in steps over whole raft area. In order to simulate the construction process, the total load is applied in increments linearly within a construction period of 360 days (12 months) and is kept constant thereafter. In the third and final phase, for an additional 1080 days (36 months), a fully coupled flow-deformation analysis is performed where a drawdown in the GWL from the ground surface up to the depth of 15 m has been considered. The maximum depth of the GWL of 15 m corresponds to 0.5 times standard length of pile (L_p), *i.e.*, 30 m. The load-settlement behavior, raft bending moment, load-sharing between the raft and piles, and pile axial load distribution for various piled raft configurations are determined and discussed in detail based on finite element analyses. Equation (1) is used to evaluate the average settlement (w_{avg}) by evaluating the displacements at the raft center (w_{center}) and raft corner (w_{corner}). As seen in Figure 3b, at the center (section A-A) of raft, the bending moment has been evaluated. The piled raft coefficient (α_{pr}), which is the ratio of the load the piles carry (Q_{p_pr}) to total applied load (Q_{pr}), is used to express the percentage of the total applied load carried by the piles, as shown in equation (2). The pile axial load is observed for piles at middle, edge, and corner locations (Figure 3b).

$$w_{avg} = \frac{1}{3}\left(2w_{center} + w_{corner}\right) \quad (1)$$

$$\alpha_{pr} = \frac{Q_{p\_pr}}{Q_{pr}} \quad (2)$$

Table 2: Different foundation parameters of the piled raft

Parameters	Values	Units
Raft dimensions ($B_r \times B_r$)	38 × 38	m
Pile number (N_p)	25, 49*, 81	-
Pile spacing (s)	4, 5, 6*	m
Corresponding piled area ratio (A_g/A_r)	0.4, 0.6, 0.9*	-
Pile length (L_p)	20, 25, 30*	m
Pile diameter (D_p)	1	m
Raft thickness (t_r)	1, 2*, 3	m
Corresponding raft-soil stiffness ratio, k_{rs}	0.08, 0.61*, 2.06	-

*Standard value if not varied

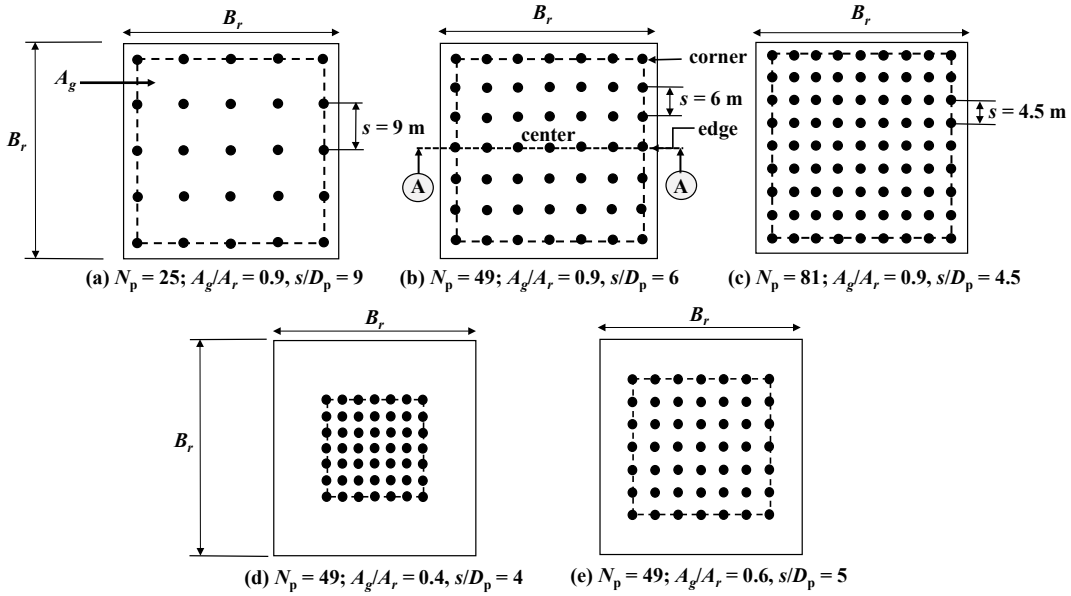

Figure 3: Different pile configurations

Table 3: Material properties and flow parameters

Materials	Properties	Values	Units
Soil	Unit weights, γ_{unsat}/ γ_{sat}	20/20	kN/m^3
	Ref. secant stiffness, E_{50}^{ref}	3.5×10^4	kN/m^2
	Ref. oedometer stiffness, E_{oed}^{ref}	4.28×10^4	kN/m^2
	Ref. unloading-reloading stiffness, E_{ur}^{ref}	1.05×10^5	kN/m^2
	Stress dependency power, m	1	-
	Poisson's ratio, v_s	0.2	-
	Cohesion, c'	20	kN/m^2
	Internal friction angle, ϕ'	20	degree
	Lateral earth pressure coefficient, K_o	0.8	-
	Specific gravity, G	2.75	-
	Liquid limit, w_L	70	(%)
	Water content, w	32	(%)
	Plasticity index, I_p	45	(%)
	Consistency index, I_c	0.9	-
	Degree of saturation, S_r	0.94	-
	Activity, I_a	1	-
Raft	Young's modulus, E_r	34,000	MN/m^2
	Poisson's ratio, v_r	0.2	-
	Unit weight	25	kN/m^3
	Buoyant unit weight	15	kN/m^3
Piles	Young's modulus, E_p	30,000	MN/m^2
	Poisson's ratio, v_p	0.2	-
	Unit weight	25	kN/m^3
	Buoyant unit weight	15	kN/m^3
Flow parameters (Van Genuchten Model)	Permeability, K	2.6×10^{-4}	m/day
	Residual saturation, S_{res}	0.18	-
	Saturated saturation, S_{sat}	1.0	-
	Fitting parameter, g_a	0.8	1/m
	Fitting parameter, g_n	1.09	-
	Fitting parameter, g_l	0.5	-

6. RESULTS AND DISCUSSIONS

7. Varying pile number

In this section, Figure 4 demonstrates the effect of loading and GWL drawdown on the overall piled raft behavior with changing pile number. Figure 4a illustrates that for a higher pile number, the average settlement is always lower for the loading period and during the GWL drawdown. This is due to the increase in the overall stiffness of the foundation with increasing pile number. The figure shows that for all configurations, the average settlement increases noticeably due to the drawdown in GWL, with a minimum increase noted for the 9 × 9 pile configuration. This is because a drop in the GWL results in the subsidence of the ground surface, indicating the consolidating behavior of the soil. Phoban *et al*. (2021) have reported similar observations due to the drawdown in the GWL but for single piles. Figure 4b illustrates the bending moment in case of different piled raft configurations at end of loading and after GWL drawdown. The raft bending moment for a piled raft with a higher pile number is always lesser than for a lower pile number piled raft due to the increased pile support underneath the raft. The drop in GWL causes the raft bending moment to decrease considerably for all the piled raft configurations with varying pile numbers. The percentage reduction in the maximum bending moment (positive) is the highest for the 9 × 9 pile configuration. The decrease in bending moment is on account of a greater raft-soil contact pressure with the GWL drawdown. Interestingly, for 81 piles (9 × 9), the bending moment is almost negligible after the drop in GWL.

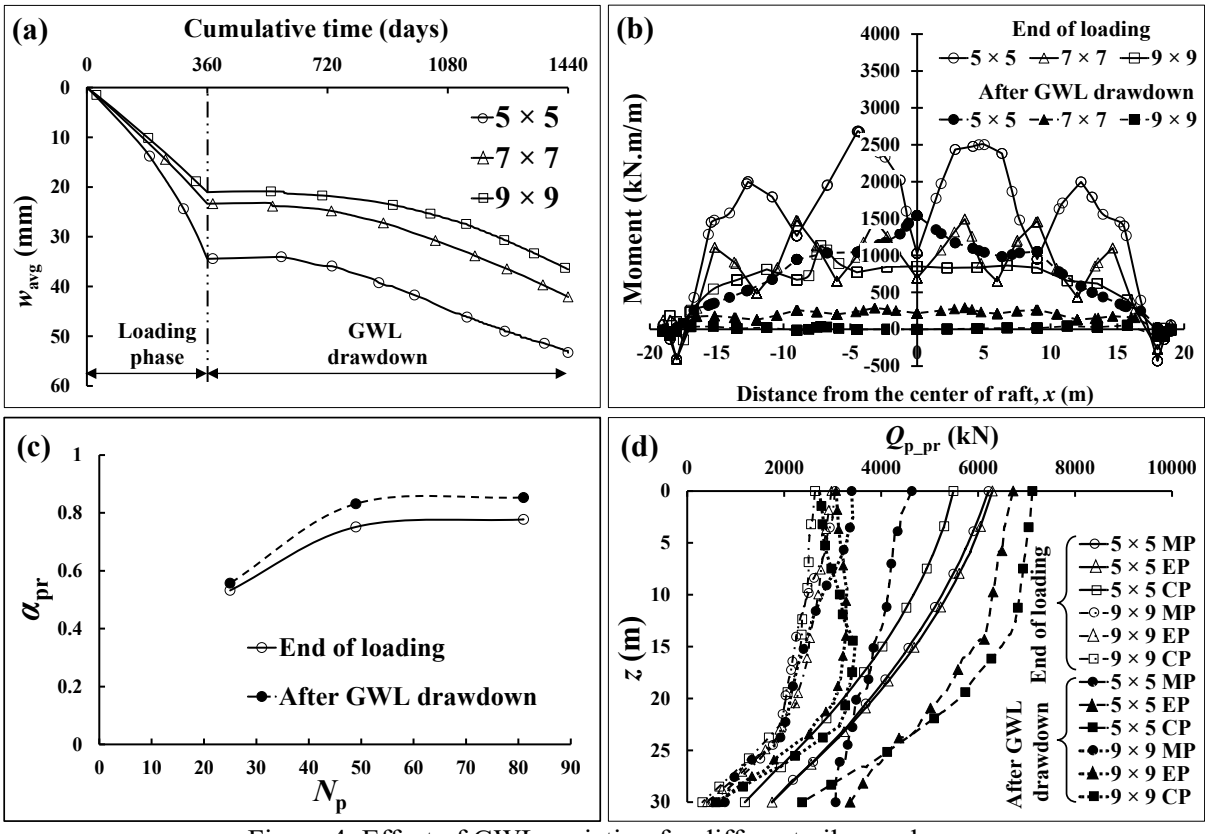

Figure 4: Effect of GWL variation for different pile numbers

Figure 4c demonstrates the variation of the piled raft coefficient (α_{pr}) with increasing pile number at the end of loading and after the GWL drawdown. As expected, with the increase in the pile number, as the pile group stiffness increases, a higher α_{pr} value is noted. It can be observed that for any pile number, due to the fall in the GWL, the α_{pr} value increases slightly. This is due to a greater mobilization of pile frictional resistance on account of the subsidence of the ground surface and consolidated soil behavior. The axial load distributions along the pile length for the middle pile (MP),

edge pile (EP), and corner pile (CP) are presented in Figure 4d. For convenience, the pile axial load distribution is presented only for the 5 × 5 and 9 × 9 pile configuration piled rafts. It can be seen that at the end of loading and after the GWL drawdown, the axial load carried by the piles at any location is lower for a higher number of piles. This is due to the fact that for a higher pile number, the total applied load is distributed to a larger number of piles. For the 5 × 5 configuration, as GWL falls, axial load carried by the EP and CP increases on account of greater mobilization of pile capacity. However, for the MP, the axial load decreases up to the depth of 0.75 L_p because of the negative skin friction encountered with the drawdown in the GWL. For the 9 × 9 piles configuration, the axial load carried by the piles at any location increases due to the fall in GWL.

8. Varying pile spacing

The influence of loading and GWL drawdown on piled raft behavior for standard 7 × 7 configuration with varying pile spacing is illustrated in Figure 5. Figure 5a shows that for the loading phase and during the GWL drawdown, the average settlement is always higher for a lower pile spacing. This is because of the pile group effect that is encountered in the case of a closer pile spacing that limits the mobilization of pile capacities. For any pile spacing, the average settlement increases due to the drawdown in GWL, with a minimum increase noted for the s/D_p ratio of 4. For s/D_p ratios of 5 and 6, the settlement values due to drawdown are almost comparable. The bending moment distributions for piled rafts with various pile spacings **at the end of loading and after the GWL drawdown** are illustrated in Figure 5b. In the figure, the negative bending moment indicates the hogging nature of raft and the positive moment implies raft sagging. Hogging raft moments are structurally unstable and thus not recommended. At the end of loading and after the fall in GWL, for s/D_p ratio of 4, a predominant hogging raft behavior is noted, and with a further increase in the s/D_p ratio the raft bending nature changes to sagging. The presence of a centrally concentrated pile support beneath the raft at a lower pile spacing to withstand the overcoming *UDL* results in the hogging raft behavior. It can be noted that for any pile spacing due to the GWL drawdown, both the positive and negative bending moments are reduced.

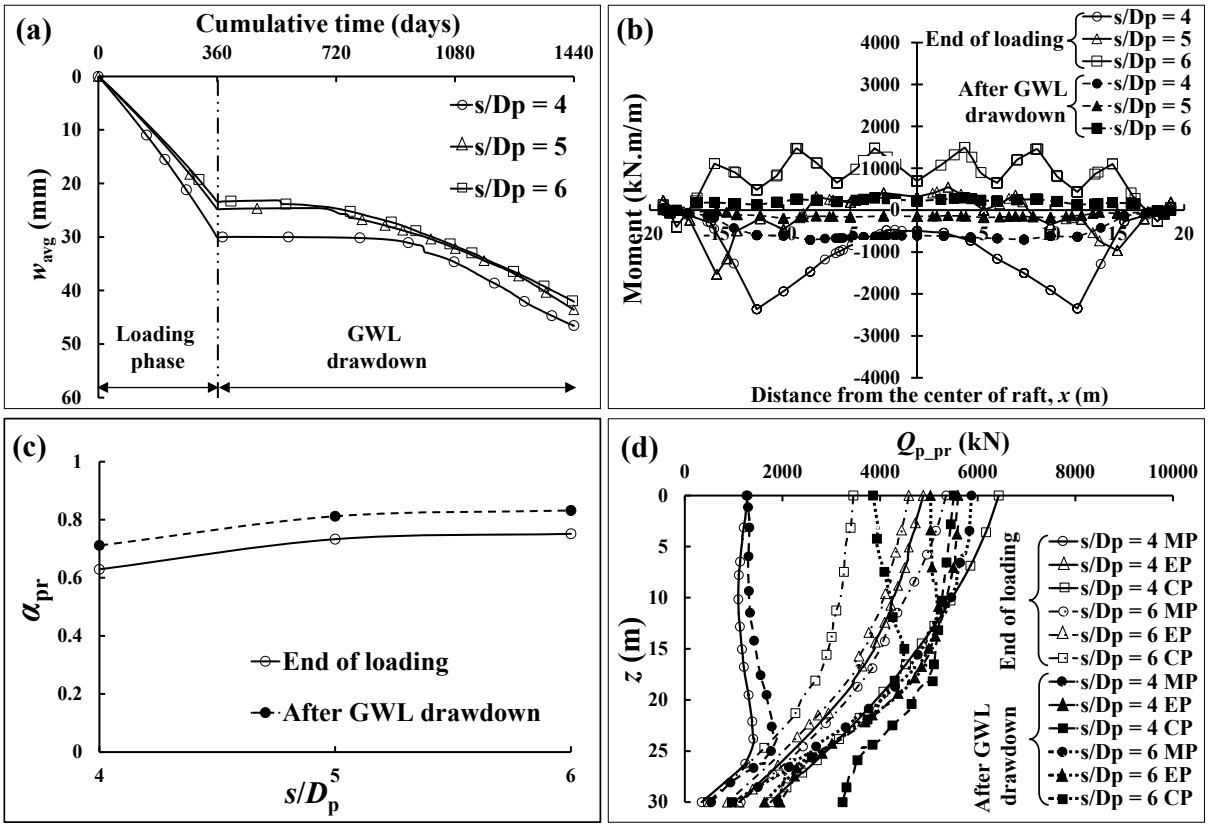

Figure 5: Effect of GWL variation for different pile spacings

For any pile spacing, Figure 5c demonstrates that the fall in the GWL increases the total load piles carry by an equal proportion. The pile axial load distributions along the pile length at the end of loading and after GWL drawdown for piled rafts with different s/D_p ratios are shown in Figure 5d. For ease, only s/D_p ratios of 4 and 6 are presented in the figure. At the end of loading, for s/D_p ratio of 4, the MP carries the minimum load and CP carries the maximum. However, for s/D_p ratio of 6, a trend reversal is noted with MP carrying the highest and CP carrying the lowest load. At the end of loading phase, Lee *et al*. (2010) have also reported that at smaller pile spacing the MP carries is minimum load than the other piles. It can be seen that for the s/D_p ratio of 4, a drop in the GWL increases the axial load carried by the MP and EP only. However, as the GWL falls, the axial load for the CP reduces up to 0.5 L_p compared to the pile axial load at the end of loading due to negative skin friction. For s/D_p ratio of 6, the pile axial load increases due to the GWL drawdown for piles positioned at any location. After the GWL drawdown, the MP carries the maximum load for a wider pile spacing but the minimum load for a closer pile spacing.

9. Varying pile length

The influence of loading and GWL drawdown on the overall foundation behavior with the standard 49 piles of varying pile lengths is illustrated in Figure 6. Figure 6a shows that an increase in the pile length (L_p/D_p ratio) results in a lower average settlement during the loading phase and GWL drawdown. A longer pile length is associated with a higher pile capacity, resulting in a lower foundation settlement. The average settlement due to the GWL drawdown is almost similar for the considered L_p/D_p ratios. This indicates that the pile length variation has no significant effect on the settlement that occurs due to the GWL drop. From the bending moment distribution, as presented in Figure 6b, it can be noted that the positive bending moment reduces slightly with the increment in pile length and substantially due to the drawdown in GWL. The decrease in the bending moment in case of longer-length piles is associated with the increased pile support in terms of pile capacity underneath the raft. However, for any length, the reduction in the bending moment due to the GWL drawdown is related to a higher raft-soil contact pressure. The percentage reduction in the maximum positive raft bending moment is the highest for L_p/D_p ratio of 30. Figure 6c illustrates that the increase in pile length increases the α_{pr} value. At the end of loading phase, similar findings for the correlation between load carried by the piles and pile length have also been reported by Lee *et al*. (2010). Also, for any pile length, the drawdown in GWL results in a higher α_{pr} value. However, it can be observed that for shorter-length piles (L_p/D_p ratio of 20), the increase in the α_{pr} value due to the drawdown in GWL is negligible. This is on account of the reduction in the pile capacities due to negative skin friction for piles located at the central raft area and near the raft edges. Figure 6d shows the pile axial load distribution at the end of loading and after GWL drawdown for L_p/D_p ratios of 20 and 30. It can be seen that for the L_p/D_p ratio of 20, the pile axial loads for the MP and EP reduce up to the depth of $0.87L_p$ and $0.47L_p$, respectively, due to the negative skin friction after the GWL drawdown. The increase in the pile axial load is observed for the CP only due to the drawdown. For longer-length piles (L_p/D_p ratio of 30), irrespective of the pile locations, the pile axial loads after the GWL drawdown are always higher compared to the axial load at the end of loading. After the GWL drawdown, the CP carries the maximum load for shorter-length piles, followed by the EP and MP. However, a trend reversal is noted for longer-length piles, with maximum load carried by MP and the CP carrying minimum load after the drop in GWL.

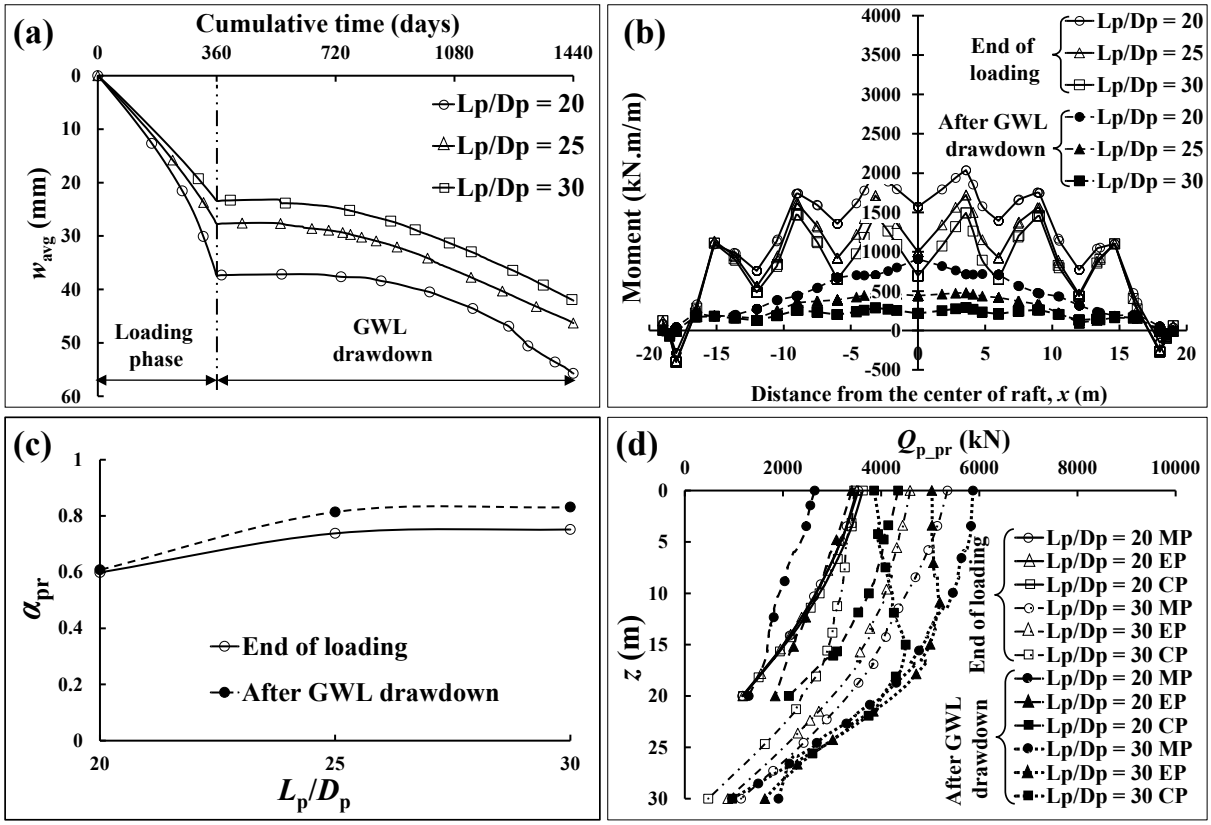

Figure 6: Effect of GWL variation for different pile lengths

10. Varying raft thickness

Figure 7 presents the effect of loading followed by the GWL drawdown for the standard 7 × 7 piled raft foundation with the raft thickness varying as 1, 2, and 3 m. Based on raft-soil stiffness ratio (k_{rs}) of 0.8, 0.6, and 2.0, the considered raft thickness values of 1, 2, and 3 m correspond to a fully flexible, flexible, and rigid raft. It can be observed from Figure 7a that a change in the raft thickness has no noticeable effect on the average settlement of the piled raft during the loading phase and drawdown of GWL. Poulos (2001) has also stated no noticeable effect of the change in the raft thickness on the average settlement. Figure 7b illustrates that for a greater thickness, positive bending moments are substantially higher at the end of the loading phase, and marginally higher after the GWL drawdown. For any raft thickness, the fall in the GWL significantly reduces the raft bending moment compared to the bending moment at the end of loading. The percentage reduction in the maximum bending moment (positive) is the highest for rigid raft (t_r = 3 m). Interestingly, for the raft thickness of 1 m, the raft bending moment is almost negligible after the GWL drawdown. As the thickness increases, the load proportion carried by piles reduces at the end of loading and after the drawdown, as shown in Figure 7c. The reduction in pile load proportion is caused by an increase in raft stiffness for a thicker raft, which draws a higher load than the group piles. The GWL drawdown causes the α_{pr} value to increase for all raft thicknesses in comparison to the α_{pr} value at the end of loading, with a slightly larger increase observed for a thicker raft. Figure 7d illustrates the distribution of pile axial load located at middle, edge, and corner locations of the piled raft with different raft thicknesses. For convenience, the results are presented for fully flexible (t_r = 1 m) and rigid raft (t_r = 3 m) cases. The figure shows that the axial load carried by the piles at any location increases for both the raft stiffnesses due to the drawdown in GWL. For fully flexible raft (t_r = 1 m), after the drawdown in the GWL, the maximum load is carried by the MP, followed by the EP and CP. However, in the case of the rigid raft (t_r = 3 m), the MP carries the minimum load, and the pile axial load variation along the length is almost similar for the EP and CP.

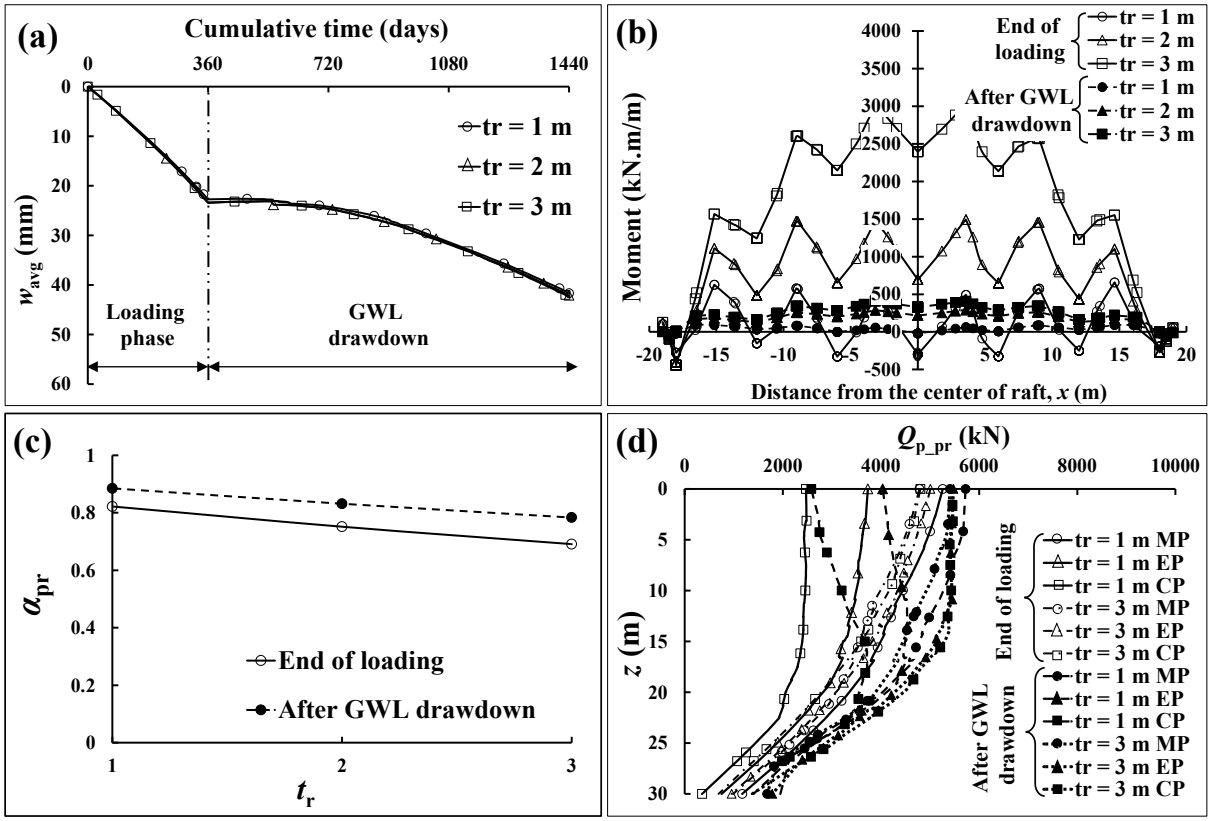

Figure 7: Effect of GWL variation for different raft thicknesses

11.CONCLUSIONS

In the study, to investigate the effect of the drawdown in GWL, three-dimensional modeling on large piled rafts in stiff clay soil has been performed with varying number, spacing, and length of piles along with different raft thicknesses. Based on the results obtained from the study, the following conclusions are drawn:

- The average settlement value at the end of loading and after the GWL drawdown is lesser for a higher pile number, wider pile spacing, or longer-length piles; however, the change in the settlement value is negligible for varying raft thickness. For any configuration, the average settlement increases due to the GWL drawdown. The increase in the settlement value due to the fall in GWL is the minimum for a higher pile number or lower pile spacing, and remains almost similar for varying pile length or raft thickness.
- The positive raft bending moment at the end of loading reduces with the increase in the pile number or pile length; however, the bending moment increases with the increase in the raft thickness. With the increase in the pile spacing the raft bending moment changes from negative to positive. Similar trends in the raft bending moments are observed after the drawdown in GWL. Both positive (sagging) and negative (hogging) raft bending moments reduce significantly due to the GWL drawdown. The percentage reduction in the maximum positive raft moments is observed to be the highest for piled raft configurations with a larger pile number, longer-length piles, or a thicker raft. For varying pile spacing, a predominant sagging raft behavior is noted only when piles are located such that they cover the maximum raft area.
- At the end of loading and after the GWL drawdown, the piled raft coefficient is higher for a larger pile number, wider pile spacing, or longer-length piles. However, the pile raft coefficient decreases with a greater raft thickness. The proportion of the total load carried by the piles increases due to the GWL drawdown. The increase in the pile load proportion is marginal for a lesser pile number or shorter length piles. However, for any pile spacing, the increase in the total load carried by the piles due to the drawdown is almost the same, and for varying raft thickness, the increase is slightly higher for a thicker raft.

- The axial load for piles at middle, edge, and corner locations increases due to the drawdown in the GWL only for a higher pile number, wider pile spacing, or longer-length piles. However, because of the GWL drawdown, the axial load the piles carry at different locations increases for any thickness of the raft. A decrease in the pile axial load after the GWL drawdown for the other cases is encountered on account of negative skin friction.

ACKNOWLEDGEMENTS

The authors acknowledge the Department of Civil Engineering, Indian Institute of Technology Guwahati, India, for providing the necessary computing facilities.

REFERENCES

Al-Khazaali, M., & Vanapalli, S. K. (2019). Experimental investigation of single model pile and pile group behavior in saturated and unsaturated sand. *Journal of Geotechnical and Geoenvironmental Engineering*, *145*(12), 04019112.

Biot, M. A. (1941). General theory of three-dimensional consolidation. *Journal of applied physics*, *12*(2), 155-164.

Brinkgreve, R., Swolfs, W., & Engin, E. (2015). PLAXIS user's manual, version 6.1. Balkema, Rotterdam, The Netherlands.

Carsel, R. F., & Parrish, R. S. (1988). Developing joint probability distributions of soil water retention characteristics. *Water Resources Research*, *24*(5), 755-769.

Cho, J., Lee, J. H., Jeong, S., & Lee, J. (2012). The settlement behavior of piled raft in clay soils. *Ocean Engineering*, *53*, 153-163.

El-Mossallamy, Y. (2002). Innovative Application of Piled Raft Foundation in stiff and soft subsoil. In *Deep Foundations 2002: An International Perspective on Theory, Design, Construction, and Performance*, 426-440.

Engin, H. K., & Brinkgreve, R. B. J. (2009). Investigation of pile behaviour using embedded piles. In *Proceedings of the 17th International Conference on Soil Mechanics and Geotechnical Engineering Alexandria,* 1189-1192.

Fraser, R. A., & Wardle, L. J. (1976). Numerical analysis of rectangular rafts on layered foundations. *Geotechnique*, *26*(4), 613-630.

Georgiadis, K., Potts, D. M., & Zdravkovic, L. (2003). The influence of partial soil saturation on pile behaviour. *Geotechnique*, *53*(1), 11-25.

Katzenbach, R., Arslan, U., & Moormann, C. (2000). Piled raft foundation projects in Germany. In *Design applications of raft foundations*, 323-391.

Lee, J., Kim, Y., & Jeong, S. (2010). Three-dimensional analysis of bearing behavior of piled raft on soft clay. *Computers and Geotechnics*, *37*(1-2), 103-114.

Park, D., Kim, I., Kim, G., & Lee, J. (2017). Groundwater effect factors for the load-carrying behavior of footings from hydraulic chamber load tests. *Geotechnical Testing Journal*, *40*(3), 440-451.

Phoban, H., Seeboonruang, U., & Lueprasert, P. (2021). Numerical modeling of single pile behaviors due to groundwater level rising. *Applied sciences*, *11*(13), 5782.

Poulos, H. G. (2001). Piled raft foundations: design and applications. *Geotechnique*, *51*(2), 95-113.

Reul, O., & Randolph, M. F. (2004). Design strategies for piled rafts subjected to nonuniform vertical loading. *Journal of Geotechnical and Geoenvironmental Engineering*, *130*(1), 1-13.

Roh, Y., Kim, I., Kim, G., & Lee, J. (2019). Comparative analysis of axial load capacity for piled-raft foundation with changes in groundwater level. *KSCE Journal of Civil Engineering*, *23*, 4250-4258.

Russo, G. & Viggiani, C. (1998). Factors controlling soil-structure interaction for piled rafts. In *International Conference on Soil-Structure Interaction in Urban Civil*, Vol. 4, 297-322. Darmstadt University.

Shahriar, M.A., Sivakugan, N., Urquhart, A., Tapiolas, M., & Das, B.M. (2013). A study on the influence of ground water level on foundation settlement in cohesionless soil. In *The 18th International Conference on Soil Mechanics and Geotechnical Engineering*, 216-229.